JACS
JOURNAL OF THE AMERICAN CHEMICAL SOCIETY
Communication
pubs.acs.org/JACS

Li Intercalation into 1D TiS_2(en) Chains

Tianyang Li,[‡] Yi-Hsin Liu,[‡] Basant Chitara, and Joshua E. Goldberger*

Department of Chemistry and Biochemistry, The Ohio State University, Columbus, Ohio 43210, United States

Supporting Information

ABSTRACT: The intercalation of metal cations in 2D layered materials allows for the discovery of unique electronic, magnetic and correlated properties. We demonstrate that reversible Li intercalation is also achievable in the hybrid organic/inorganic dimensionally reduced 1D van der Waals solid TiS_2(ethylenediamine). Upon intercalation, electrons are injected into the lattice as Ti^{4+} is reduced to Ti^{3+} leading to an order of magnitude decrease in electrical resistivity. This reversible intercalation process opens up new opportunities to fine-tune the physical properties in this emerging family of dimensionally reduced materials.

The intercalation of polymers, small molecules, and metals inside the van der Waals gap of 2D solids is one of the most powerful approaches for tuning the electronic, magnetic, and correlated properties to realize interesting physical phenomena and applications.[1] For example, it has been well established that metals can be intercalated inside layered transition metal dichalcogenides (LMDCs) to create superconductors,[2,1s] thermoelectric materials,[3] charge density waves,[4] and Li ion battery electrodes.[5] Li intercalation in these LMDCs reduces the chalcogenide host, with the electrons filling the metal d-orbital based conduction band, with the resulting Li^+ resides on the octahedral hole sites in the van der Waals gap.[6a,1d,6b] The feasibility of Li intercalation in the narrow band gap semiconductor, TiS_2, made it one of the first Li battery cathode material candidates.[7]

There is an emerging body of work suggesting that the polyhedral connectivity of atoms for *any* crystalline framework can be ligand-terminated along specific axes to produce stable, crystalline dimensionally reduced van der Waals solids that have single to few atom thicknesses.[8] These dimensionally reduced derivatives have fundamentally different properties, compared to the original lattice, such as conversion from indirect to direct band gaps,[8e] efficient white light emission,[9] and unique magnetic behavior.[10] Being able to intercalate metal cations and donate electrons inside a dimensionally reduced hybrid lattice could similarly enable the rational manipulation of their electronic and magnetic properties. Still, the intercalation and deintercalation of metal cations inside a dimensionally reduced hybrid organic/inorganic lattice has yet to be demonstrated. Herein, we show that 1 equivalent of Li can be intercalated inside TiS_2(en) (en = ethylendiamine), a dimensionally reduced 1D transition metal dichalcogenide derivative, which reduces the Ti^{4+} framework to Ti^{3+}, and leads to a significantly enhanced electrical conductivity.

We have recently created TiS_2(en), the dimensionally reduced one-dimensional (1D) derivative of a layered metal dichalcogenide lattice.[8e] TiS_2 normally crystallizes into the $CdCl_2$ structure type, consisting of layers of edge sharing TiS_6 octahedra. The TiS_2(en) lattice is derived by removing four of the six neighboring octahedra in a single layer, resulting in 1D zigzag edge sharing chains. The two nonedge-sharing S atoms on each Ti−S octahedron are substituted with a bidentate en ligand. The chains are twisted into a threefold helicity, and held together via van der Waals forces (Figure 1a). The crystal structures were determined using Rietveld refinements of 2 K neutron diffraction data which will be described further. The 0.3 eV indirect band gap[11] of TiS_2 is converted into a 1.7 eV direct band gap in TiS_2(en).

TiS_2(en) was prepared by the 220 °C solvothermal reaction of $TiCl_4$, elemental S, and en, and subsequently purified and crystallized in 2-propanol. Pure TiS_2(en) forms a unit cell with $R\bar{3}c$ symmetry (room temperature: a = 18.596(1) Å, c = 9.0158(1) Å). The narrow full width half-maximum (fwhm) (0.0014(3) rad for the (110) reflection) in the powder X-ray diffraction (XRD) pattern is indicative of its large (>500 nm) crystalline domain size. For intercalation, the TiS_2(en) product was dispersed in hexane (dried using molecular sieves prior to use) in a glovebox, and stoichiometric equivalents of *n*-butyl Lithium (*n*-BuLi) dissolved in hexane were added to the mixture. The reaction mixture was sealed, removed from the glovebox and reacted at 50 °C for 1−2 days, and then the final product was collected via centrifugation and purified with hexane. The final product is *extremely* air and water-sensitive and all subsequent analyses were performed under inert Ar atmospheres. After Li intercalation, the $R\bar{3}c$ unit cell was still observed in the XRD pattern; however, there was a noticeable shift in most of the observed reflections to lower 2θ values (Figure 1b,c). The unit cell parameters, determined via a Lebail analysis, showed a large expansion (~0.6 Å) in the a and b direction and a slight contraction (~0.07 Å) in c direction after reaction with 1 full equiv of *n*-BuLi. The expansion or contraction in the unit cell parameters is proportional to the number of equivalents of Li in the lattice (Figure 1d). Additionally, after Li incorporation the fwhm of the diffraction peaks increases (0.0030(3) rad for the (110) reflection). The strong correlation between fwhm broadening and 2θ is indicative of lattice strain as deduced via Williamson-Hall plot (Figure SI-1). Furthermore, the strain increases with increasing Li intercalation stoichiometry. The Li:Ti ratios were further verified with Inductively Coupled Plasma-Optical Emission Spectroscopy measurements.

Received: December 30, 2013
Published: February 12, 2014

dx.doi.org/10.1021/ja4132399 | *J. Am. Chem. Soc.* 2014, 136, 2986−2989

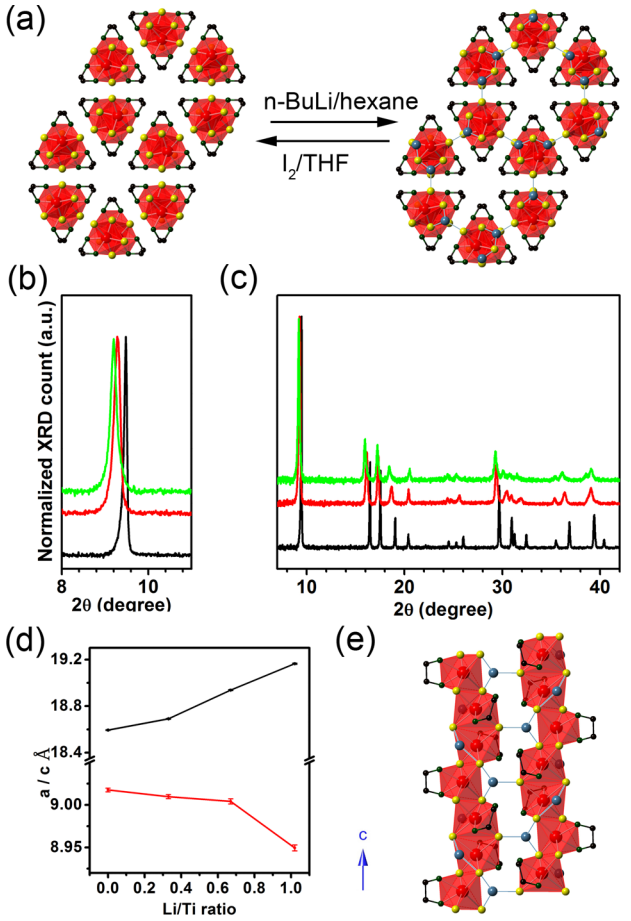

Figure 1. (a) Crystal structures of TiS_2(en) (left) and $LiTiS_2$(en) (right) projected down the *c* axis from neutron diffraction refinements. Ti octahedra are shaded in red. (b, c) X-ray diffraction patterns of TiS_2(en) (black), $Li_{0.66}TiS_2$(en) (red), and $LiTiS_2$(en). (d) Changes of unit cell parameter (*a*, black; *c*, red) with respect to Li/Ti ratio. (e) Crystal structures showing two adjacent 1D chains along *c* axis with intercalated Li atoms positions determined from neutron diffraction refinements. Atom colors: Ti, red; S, yellow; N, green; C, black. H atoms have been omitted for clarity.

To elucidate the structure and the Li atom positions, we used separate synchrotron and neutron diffraction measurements. Rietveld refinement of the synchrotron data shows that upon intercalation the interchain spacing increases from 6.151 to 6.380 Å, suggesting Li intercalation between the chains (Figure SI-2). The reduction in the *c* parameter occurs due to the increased tilting of Ti octahedra. Furthermore, upon Li intercalation the Ti−S and Ti−N bond distances increase by ∼0.11 and ∼0.03 Å, respectively (Table SI-1). The bond valence sum of Ti in TiS_2(en) and $LiTiS_2$(en) is 3.93 and 3.10,[12] respectively, further confirming the reduction of the Ti. To determine the positions of the Li atoms, we did Rietveld refinement from time-of-flight neutron diffraction measurements (Figure SI-3). Li refines to the van der Waals gap between neighboring chains, and is coordinated by three S atoms (Figure 1e). The Li−S distances are 2.227(6) and 2.231(1) Å. The bond valence sum of Li in $LiTiS_2$(en) is 1.31, which suggests that Li has a +1 oxidation state.

The Li^+ ions can be further deintercalated while preserving the structure by oxidizing the lattice. As-prepared $LiTiS_2$(en) was dispersed in a THF solvent with stoichiometric equivalents of I_2 to oxidize the lattice. The product was then repeated washed in THF to remove the LiI. The XRD data for samples before and after intercalation and after deintercalation is shown in Figure 2a. The structure and lattice parameters of the sample after deintercalation are the same as the original TiS_2(en), confirming the reversibility of intercalation.

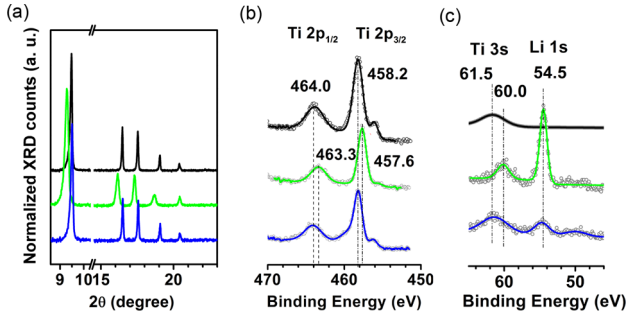

Figure 2. (a) Shift of peaks in the X-ray diffraction patterns. (b) Changes of binding energy of Ti during reversible Li intercalation. (c) Changes of Li peaks during reversible Li intercalation. Black, TiS_2(en); green, Li intercalated TiS_2(en); blue, deintercalated TiS_2(en).

X-ray photoelectron spectroscopy (XPS) was used to determine if Ti^{4+} is reduced to Ti^{3+} upon intercalation. In TiS_2(en) Ti, S, C, and N peaks were observed, but upon intercalation, only the Ti peak energies were significantly changed. Figure 2b shows the changes in Ti peaks upon intercalation and deintercalation. TiS_2(en) has Ti $2p_{1/2}$ and $2p_{3/2}$ peaks occurring at 464.0 and 458.2 eV, which is indicative of a Ti^{4+} oxidation state.[13] Additionally, there is a small shoulder at 456.0 eV indicative of reduced Ti states. We suspect that this is due to some surface S atomic desorption in the ultrahigh vacuum environment. Ar ion etching could not produce a clean stoichiometric surface and instead all of the peaks in the XPS spectrum were broadened after etching. Upon Li intercalation, the Ti peaks shift by ∼0.7 eV, which is indicative of a change in oxidation state to Ti^{3+}.[14,5e] Furthermore, the Ti 3s peak that originally occurs at 61.5 eV is shifted to 60.0 eV upon Li intercalation,[15] along with the appearance of a Li 1s peak at 54.5 eV[16] (Figure 2c). This is relatively close to the reported binding energy of Li^+ in Li_2S.[17] After treatment with I_2/THF, the Ti peaks shift back to the energies observed in TiS_2(en), and the Li 1s peak almost completely disappears. The Li residual in the structure is estimated to be 7.4% after comparing the Li XPS peak areas before and after deintercalation. This confirms that the Ti^{4+} ion is indeed reduced to Ti^{3+} upon Li intercalation.

TiS_2(en) is a 1.7 eV direct band gap semiconductor. Upon Li intercalation, one would expect the conduction band to start filling, resulting in a significantly enhanced carrier concentration and lower resistivity values. To probe changes in electrical conductivity upon lithium intercalation, we prepared two-probe current−voltage (IV) measurements of ∼5 μm thick films of TiS_2(en) on glass substrates (Figure 3a). Top-contact metal electrodes consisting of 650 nm of Ti and 20 nm of Au and separated by 10 μm lengths were defined by electron beam evaporation through a shadow mask (Figure 3b). The average two-probe resistivity of at least 10 TiS_2(en) was measured to be $\sim 2.6 \times 10^7$ Ω·cm (Figure 3c). Then the device was placed in excess *n*-BuLi hexane solution for 1 day, rinsed with hexane and the conductivity was remeasured using the same contact pads, in order to minimize deviations due to variations in film

dx.doi.org/10.1021/ja4132399 | J. Am. Chem. Soc. 2014, 136, 2986−2989

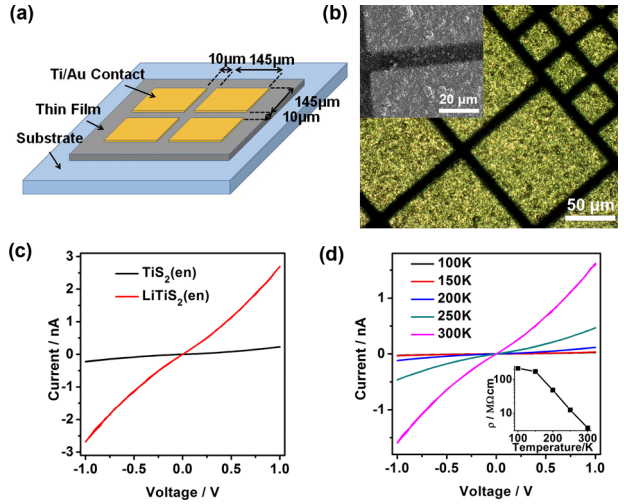

Figure 3. (a) Simplified illustration of the thin film device (not drawn to scale). (b) Optical microscope image of one $TiS_2(en)$ thin film device; insert: scanning electron microscope image of two contacts on the thin film. (c) IV curves of $TiS_2(en)$ and $LiTiS_2(en)$ in dark and Ar atmosphere. (d) IV curves of $LiTiS_2(en)$ at different temperatures; insert: resistivity vs temperature plot.

thickness and particle−particle contacts. Upon Li intercalation, the resistivity decreased by greater than 1 order of magnitude to 2.1×10^6 Ω·cm (Figure 3c). A 12- to 15-fold decrease in resistivity was observed for four different regions on the same film. This decrease in resistivity upon Li intercalation is most likely due to the enhanced carrier concentration upon doping. The resistivity of $LiTiS_2(en)$ still increases upon cooling, indicative of semiconducting behavior (Figure 3d). It is important to point out that the resistivity values measured from this 2-probe approach represent an upper bound of the material's resistivity, since they neglect the influence of contact resistances that are evident from the non-ohmicity of the IV curves.

In summary, we have successfully shown that it is possible to reversibly intercalate up to 1 full equivalent of lithium inside this dimensionally reduced hybrid organic/inorganic 1D lattice of $TiS_2(en)$. Upon Li intercalation, the Ti^{4+} is reduced to Ti^{3+}, and the conductivity of $TiS_2(en)$ increases by at least an order of magnitude. The ability to tune the electron count of hybrid organic/inorganic dimensionally reduced systems provides a pathway for the emergence of new physical phenomena, and could potentially impact existing technologies such as charge storage applications. For example, one could now explore how molecular-scale dimensionality affects the voltage, kinetics, and capacity of Li ion storage, comparing TiS_2 and $TiS_2(en)$ as model electrode materials. More generally, we foresee the ability to intercalate different kinds of atoms into dimensionally reduced materials to be a powerful strategy to yield fundamentally new behavior.

■ ASSOCIATED CONTENT

Supporting Information

Structural details and synchrotron and neutron diffraction patterns and refinement results. This material is available free of charge via the Internet at http://pubs.acs.org.

■ AUTHOR INFORMATION

Corresponding Author

goldberger@chemistry.ohio-state.edu

Author Contributions

‡T.L. and Y.-H.L. contributed equally.

Notes

The authors declare no competing financial interest.

■ ACKNOWLEDGMENTS

We acknowledge M. Suchomel (11-BM) for the assistance in collecting XRD at the Advanced Photon Source at Argonne National Laboratory, which is supported by the U.S. Department of Energy, Office of Science, Office of Basic Energy Sciences, under Contract DEAC02-06CH11357, and Ashfia Huq at POWGEN beam line 11-A, at Oak Ridge National Laboratory, and OSU NanoSystems Laboratory. J.E.G. thanks the OSU Research Foundation for financial support. Y.-H.L. thanks the National Science Council (Taiwan, R. O. C) for travel support to Oak Ridge National Lab under 102-2914-I-002-043-A1.

■ REFERENCES

(1) (a) Wertheim, G. K.; DiSalvo, F. J.; Buchanan, D. N. E. *Solid State Commun.* **1973**, *13*, 1225. (b) Schöllhorn, R.; Meyer, H. *Mater. Res. Bull.* **1974**, *9*, 1237. (c) Rijnsdorp, J.; de Lange, G. J.; Wiegers, G. A. *J. Solid State Chem.* **1979**, *30*, 365. (d) Dahn, J. R.; McKinnon, W. R.; Haering, R. R.; Buyers, W. J. L.; Powell, B. M. *Can. J. Phys.* **1980**, *58*, 207. (e) Lewerenz, H. J.; Heller, A.; DiSalvo, F. J. *J. Am. Chem. Soc.* **1980**, *102*, 1877. (f) Meerschaut, A.; Gressier, P.; Guemas, L.; Rouxel, J. *Mater. Res. Bull.* **1981**, *16*, 1035. (g) Gee, M. A.; Frindt, R. F.; Joensen, P.; Morrison, S. R. *Mater. Res. Bull.* **1986**, *21*, 543. (h) Joensen, P.; Frindt, R. F.; Morrison, S. R. *Mater. Res. Bull.* **1986**, *21*, 457. (i) Rouxel, J. *J. Solid State Chem.* **1986**, *64*, 305. (j) Friend, R. H.; Yoffe, A. D. *Adv. Phys.* **1987**, *36*, 1. (k) Divigalpitiya, W. M. R.; Frindt, R. F.; Morrison, S. R. *Science* **1989**, *246*, 369. (l) Kanatzidis, M. G.; Wu, C. G.; Marcy, H. O.; Degroot, D. C.; Kannewurf, C. R.; Kostikas, A. *Adv. Mater.* **1990**, *2*, 364. (m) Rouxel, J. *Acc. Chem. Res.* **1992**, *25*, 328. (n) England, C. D.; Collins, G. E.; Schuerlein, T. J.; Armstrong, N. R. *Langmuir* **1994**, *10*, 2748. (o) Lemmon, J. P.; Lerner, M. M. *Chem. Mater.* **1994**, *6*, 207. (p) Lemmon, J. P.; Wu, J.; Oriakhi, C.; Lerner, M. M. *Electrochim. Acta* **1995**, *40*, 2245. (q) Bissessur, R.; Heising, J.; Hirpo, W.; Kanatzidis, M. *Chem. Mater.* **1996**, *8*, 318. (r) Schöllhorn, R. *Chem. Mater.* **1996**, *8*, 1747. (s) Morosan, E.; Zandbergen, H. W.; Dennis, B. S.; Bos, J. W. G.; Onose, Y.; Klimczuk, T.; Ramirez, A. P.; Ong, N. P.; Cava, R. J. *Nat. Phys* **2006**, *2*, 544. (t) Koski, K. J.; Cha, J. J.; Reed, B. W.; Wessells, C. D.; Kong, D. S.; Cui, Y. *J. Am. Chem. Soc.* **2012**, *134*, 7584. (u) Koski, K. J.; Wessells, C. D.; Reed, B. W.; Cha, J. J.; Kong, D. S.; Cui, Y. *J. Am. Chem. Soc.* **2012**, *134*, 13773. (v) Cha, J. J.; Koski, K. J.; Huang, K. C. Y.; Wang, K. X.; Luo, W.; Kong, D.; Yu, Z.; Fan, S.; Brongersma, M. L.; Cui, Y. *Nano Lett.* **2013**, *13*, 5913.

(2) (a) Gamble, F. R.; Osiecki, J. H.; Cais, M.; Pisharod, R. *Science* **1971**, *174*, 493. (b) Tarascon, J. M.; DiSalvo, F. J.; Murphy, D. W.; Hull, G.; Waszczak, J. V. *Phys. Rev. B* **1984**, *29*, 172.

(3) (a) Chung, D. Y.; Hogan, T. P.; Rocci-Lane, M.; Brazis, P.; Ireland, J. R.; Kannewurf, C. R.; Bastea, M.; Uher, C.; Kanatzidis, M. G. *J. Am. Chem. Soc.* **2004**, *126*, 6414. (b) Guilmeau, E.; Breard, Y.; Maignan, A. *Appl. Phys. Lett.* **2011**, *99*, 052107.

(4) (a) Murphy, D. W.; Disalvo, F. J.; Hull, G. W.; Waszczak, J. V. *Inorg. Chem.* **1976**, *15*, 17. (b) van Bruggen, C. F.; Haas, C.; Wiegers, G. A. *J. Solid State Chem.* **1979**, *27*, 9.

(5) (a) Murphy, D. W.; Di Salvo, F. J.; Hull, G. W.; Waszczak, J. V. *Inorg. Chem.* **1976**, *15*, 17. (b) Murphy, D. W.; Trumbore, F. A. *J. Cryst. Growth* **1977**, *39*, 185. (c) Dahn, J.; Haering, R. R. *Mater. Res. Bull.* **1979**, *14*, 1259. (d) Murphy, D. W.; Christian, P. A. *Science* **1979**, *205*, 651. (e) Moreau, P.; Ouvrard, G.; Gressier, P.; Ganal, P.; Rouxel,

J. *J. Phys. Chem. Solids* **1996**, *57*, 1117. (f) Aydinol, M. K.; Kohan, A. F.; Ceder, G.; Cho, K.; Joannopoulos, J. *Phys. Rev. B* **1997**, *56*, 1354. (g) Gao, M. R.; Xu, Y. F.; Jiang, J.; Yu, S. H. *Chem. Soc. Rev.* **2013**, *42*, 2986.
(6) (a) Whittingham, M. S.; Gamble, F. R., Jr. *Mater. Res. Bull.* **1975**, *10*, 363. (b) Py, M. A.; Haering, R. R. *Can. J. Phys.* **1983**, *61*, 76.
(7) (a) Whittingham, M. S. *Science* **1976**, *192*, 1126. (b) Whittingham, M. S. *Chem. Rev.* **2004**, *104*, 4271.
(8) (a) Long, J. R.; McCarty, L. S.; Holm, R. H. *J. Am. Chem. Soc.* **1996**, *118*, 4603. (b) Kagan, C. R.; Mitzi, D. B.; Dimitrakopoulos, C. D. *Science* **1999**, *286*, 945. (c) Huang, X. Y.; Li, J.; Fu, H. X. *J. Am. Chem. Soc.* **2000**, *122*, 8789. (d) Mitzi, D. B. *Adv. Mater.* **2009**, *21*, 3141. (e) Liu, Y. H.; Porter, S. H.; Goldberger, J. E. *J. Am. Chem. Soc.* **2012**, *134*, 5044. (f) Morris, C. D.; Chung, I.; Park, S.; Harrison, C. M.; Clark, D. J.; Jang, J. I.; Kanatzidis, M. G. *J. Am. Chem. Soc.* **2012**, *134*, 20733.
(9) Roushan, M.; Zhang, X.; Li, J. *Angew. Chem., Int. Ed.* **2012**, *51*, 436.
(10) Pak, C.; Kamali, S.; Pham, J.; Lee, K.; Greenfield, J. T.; Kovnir, K. *J. Am. Chem. Soc.* **2013**, *135*, 19111.
(11) Chen, C. H.; Fabian, W.; Brown, F. C.; Woo, K. C.; Davies, B.; DeLong, B.; Thompson, A. H. *Phys. Rev. B* **1980**, *21*, 615.
(12) Brown, I. D. *J. Appl. Crystallogr.* **1996**, *29*, 479.
(13) (a) Blasco, T.; Camblor, M. A.; Corma, A.; Perezpariente, J. *J. Am. Chem. Soc.* **1993**, *115*, 11806. (b) Sanjines, R.; Tang, H.; Berger, H.; Gozzo, F.; Margaritondo, G.; Levy, F. *J. Appl. Phys.* **1994**, *75*, 2945.
(14) Werfel, F.; Brummer, O. *Phys. Scr.* **1983**, *28*, 92.
(15) Groenenb, C. J.; Sawatzky, G.; Deliefde, H. J.; Jellinek, F. *J. Organomet. Chem.* **1974**, *76*, C4.
(16) Chowdari, B. V. R.; Rong, Z. *Solid State Ionics* **1996**, *90*, 151.
(17) (a) Moulder, J. F.; Chastain, J. *Handbook of X-ray Photoelectron Spectroscopy: A Reference Book of Standard Spectra for Identification and Interpretation of XPS Data*, Physical Electronics Division, Perkin-Elmer Corp, 1995; (b) Seh, Z. W.; Wang, H.; Hsu, P.-C.; Zhang, Q.; Li, W.; Zheng, G.; Yao, H.; Cui, Y. *Energy Environ. Sci.* **2014**, *7*, 672.